

**CONSTRAINING ALTERATION PROCESSES ALONG THE SICCAR POINT UNCONFORMITY, GALE CRATER: RESULTS FROM THE SAMPLE ANALYSIS AT MARS INSTRUMENT.** B. Sutter<sup>1,2</sup>, A.C. McAdam<sup>3</sup>, D.W. Ming<sup>2</sup>, P.D. Archer<sup>1,2</sup>, L.M. Thompson<sup>4</sup>, J.C. Stern<sup>3</sup>, J.L. Eigenbrode<sup>3</sup>, P.R. Mahaffy<sup>3</sup>. <sup>1</sup>Jacobs, Houston, TX, [brad.sutter-2@nasa.gov](mailto:brad.sutter-2@nasa.gov), <sup>2</sup>NASA/JSC, Houston, TX, <sup>3</sup>NASA/GFSC, Greenbelt, MD, <sup>4</sup>Planetary Space Sci. Centre, Univ. New Brunswick, Canada,

**Introduction:** A driving factor for sending the Mars Science Laboratory, Curiosity rover to Gale Crater was the orbital detection of clay minerals in the Glen Torridon (GT) region suggesting a past aqueous environment that could contain organic evidence of past microbiology. The objective of the Curiosity's Sample Analysis at Mars (SAM) instrument was to detect organic evidence of past microbiology and volatile bearing mineralogy suggestive of past geochemical conditions that would have supported microbiology in the GT region.

The Siccar Point unconformity occurred between the underlying GT mudstone and the overlying Stimson sandstone of the Greenheugh Pediment. Just below the contact is evidence of enhanced alteration suggestive of aqueous processes favorable for microbial activity. The altered material may result from subaerial weathering, alteration from fluids moving along unconformity, upward fluid percolation from the mudstone or downward fluid percolation from the Pediment<sup>1,2,3,4,5</sup>

The objectives of this work were to 1) Utilize the SAM-evolved gas analyzer (EGA) results to characterize the geochemistry and mineralogy above and below the Siccar Point unconformity through analysis of drilled samples in three GT mudstones and an overlying pediment sandstone and 2) Utilize SAM-EGA results to constrain alteration scenario(s) below the unconformity.

**Materials & Methods:** The GT mudstone samples examined in this work were from the Glasgow member (Gm) and consist of the Glasgow (GG) and Nontron (NT) samples that were less altered and occur well below the unconformity (>16m) and the more altered Hutton sample (HU) that is closer to unconformity (~ 3 to 4 m). All three Gm lacustrine mudstones were believed to be initially derived from the same source material with the HU sample undergoing greater post-depositional alteration relative to GG and NT. The Edinburgh (EB) sandstone sample occurred in the Greenheugh pediment approximately 2.7 to 3.7 m above the unconformity.<sup>6</sup> The goal of this work was to constrain alteration scenarios by comparing the more altered HU material with the less altered GG and NT materials and evaluate the role Greenheugh pediment fluids may have had in altering HU through examination of the EB sample.

The SAM-EGA heated a sample (~35 °C min<sup>-1</sup>) to ~870°C where He carrier gas (~0.8 sccm; 25 mbar)

swept evolved gases from the SAM oven to the quadrupole mass spectrometer for identification. Evolved gases (e.g., H<sub>2</sub>O, SO<sub>2</sub>, CO<sub>2</sub>, etc.) evolved at characteristic decomposition temperatures of volatile bearing phases identified mineral and/or organic phases. CheMin X-ray diffraction<sup>7</sup> and Alpha Particle X-ray Spectrometer (APXS)<sup>5</sup> analyses provided supporting mineralogical and total chemical data.

**Results/Discussion:** The GG, NT, HU and EB samples evolved 1.3 to 1.7 wt% H<sub>2</sub>O with peaks at nearly similar temperatures; however variable peak intensity between samples below 300°C suggested the levels of adsorbed water and hydrated salts varied

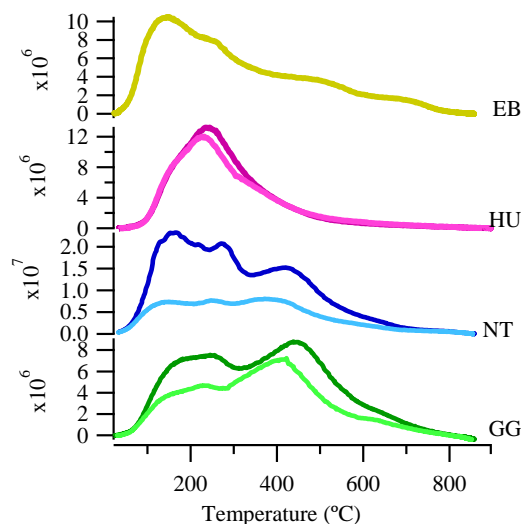


**Fig. 1. Evolved H<sub>2</sub>O versus temperature.**

between samples (Fig. 1). The main difference was that the HU lacked the peak between 400°C and 500°C that was present in the other samples (Fig. 1). This peak was due to Fe-smectite as confirmed by CheMin<sup>7</sup> and was consistent with open system acidic-alteration of HU resulting in smectite loss. The two EB sandstone H<sub>2</sub>O peaks above 500°C were consistent with Fe-smectite and Mg-smectite<sup>7</sup> consistent with EB sandstone that underwent post-depositional alteration allowing smectite formation.

Evolved SO<sub>2</sub> releases were consistent with the presence of Fe-sulfate (~ 500°C) and minor Mg-sulfate (~800°C; GG, NT only) (Fig. 2). Fe- and Mg- sulfate abundance accounted for <20% of total S indicating that Ca-sulfate dominated S in these samples. Lower SAM-S (0.25 wt.% SO<sub>3</sub>) in HU relative to GG (0.7

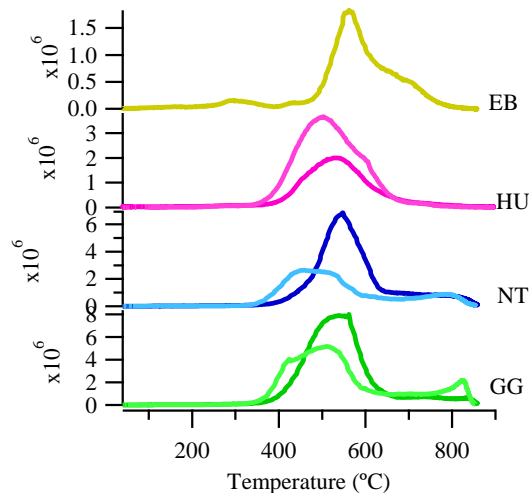


**Fig. 2. Evolved  $\text{SO}_2$  versus temperature.**

wt.%) and NT (1.2 wt.%) suggested that sulfur poor alteration fluids could have leached Fe/Mg-S phases from HU. The EB evolved S profile differed from HU as indicated by a  $\sim 300^\circ\text{C}$  peak, likely from oxidation of Fe-sulfide, and  $700^\circ\text{C}$   $\text{SO}_2$  peak not present in HU (Fig. 2). The contrasting evolved  $\text{SO}_2$  profiles between EB and HU were consistent with the lack of exchange of S bearing fluids between EB and HU.

Evolved  $\text{CO}_2$  and CO were consistent with the presence of indigenous martian carbon or carbon derived from meteoritic inputs (Fig. 3).<sup>8,9</sup> The main evolved CO and  $\text{CO}_2$  peaks ( $<500^\circ\text{C}$ ) were consistent with the presence of low molecular weight C phases (e.g., oxalates, acetates<sup>10</sup>) and carboxylated macromolecular carbon, while evolved  $\text{O}_2$  (data not shown) detected in EB may have combusted reduced C to  $\text{CO}_2$  detected in EB. Less intense  $\text{CO}_2$  and CO detections above  $600^\circ\text{C}$  were consistent with contributions from  $\text{CO}_2$  inclusions within glass phases and decarbonylation of larger organic carbon phases. Co-evolving  $\text{CO}_2$ , CO, and  $\text{SO}_2$  at  $800^\circ\text{C}$  most notably in the GG and NT samples was consistent with Mg-sulfate preservation of organic C (Figs. 2&3). The  $\text{CO}_2$  and CO carbon abundances in the GG, NT, and HU samples were variable (200 to  $700 \mu\text{gC/g}$ ) suggesting alteration processes operating in HU did not affect C abundance in HU relative to GG and NT. Differing evolved  $\text{CO}_2$  pattern between EB and HU coupled with significantly higher  $\text{CO}_2$ -C in EB ( $1500 \mu\text{gC/g}$ ) was consistent with little exchange of C between EB and the underlying HU material.

Evolved  $\text{O}_2$  and very limited NO, associated with(per)chlorate and nitrate, respectively, were not detected in Gm mudstones (GG, NT and HU) but were detected in the overlying EB sandstone (data not

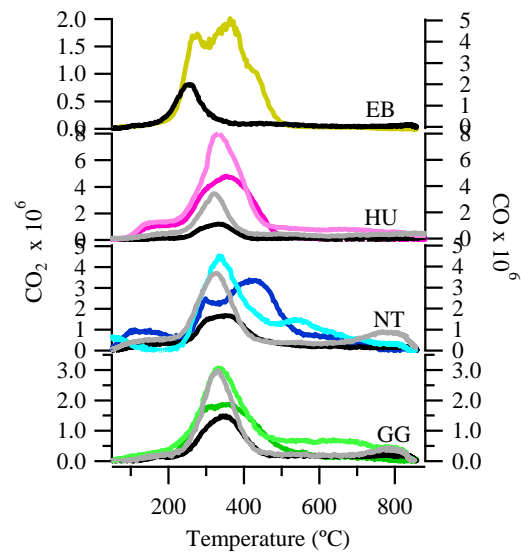


**Fig. 3. Evolved  $\text{CO}_2$  (color) and CO (black/grey) versus temperature.**

the Gm materials and underlying GT mudstones was consistent with nitrate and (per)chlorate loss after deposition in all GT mudstones or that these phases were never deposited. The presence of (per)chlorate and nitrate in EB but not HU was consistent with EB fluids never transporting these soluble salts into the underlying HU sediments.

Loss of smectite and Fe/Mg-S phases in HU relative to GG and NT were consistent with HU alteration after deposition. Alteration processes did not affect concentration of C phases in HU suggesting C contents could have experienced a mix of gains and losses during HU alteration. The contrasting evolved gas characteristics and abundances of the EB sample relative to HU did not support fluid exchange between Stimson and HU. SAM-EGA results were alone unable to further constrain the alteration scenarios relative to sub-aerial alteration, diagenetic fluid alteration along the unconformity or upward migrating fluids. Evaluation of additional data sets (e.g., Chemcam<sup>2,3,4</sup>, APXS<sup>5</sup>) suggested that diagenetic alteration along the unconformity was the favored alteration mechanism for HU.

**References:** [1]Yen, A. et al. (2021) *JGR*,126, 2020JE006569. [2]DeHouck E. et al. (2020) *LPS LI* 2770. [3]Gasda P. et al. (2021) *LPS LII*, #1271 [4]Bedford C. et al. (2021) *LPS LII*, #1569 [5]Thompson, L. et al. (2021) *LPS LII*, #241. [6]Banham et al This LPS [7]Thorpe M. et al. (2021) *LPS LII*, #1519 [8]Flynn, G(1996) *Earth Moon Plt* 72,469. [9] Steele A. et al. (2016) *Met. Plt. & Sci* 21, 2203 [10] Lewis et al. (2021) *JGR*,126, e2020JE006803.